PHYSICAL REVIEW A **83**, 031602(R) (2011)

Interferometry with synthetic gauge fields

Brandon M. Anderson, Jacob M. Taylor, and Victor M. Galitski
Condensed Matter Theory Center and Joint Quantum Institute, Department of Physics, University of Maryland, College Park, Maryland 20742-4111, USA

(Received 30 August 2010; published 3 March 2011)

We propose a compact atom interferometry scheme for measuring weak, time-dependent accelerations. Our proposal uses an ensemble of dilute trapped bosons with two internal states that couple to a synthetic gauge field with opposite charges. The trapped gauge field couples spin to momentum to allow time-dependent accelerations to be continuously imparted on the internal states. We generalize this system to reduce noise and estimate the sensitivity of such a system to be $S \sim 10^{-7}\,\frac{\mathrm{m/s^2}}{\sqrt{\mathrm{Hz}}}$.

DOI: 10.1103/PhysRevA.83.031602 PACS number(s): 03.75.Dg, 37.25.+k, 67.85.−d

In recent years atom interferometry has emerged as a powerful tool for precision gravimetry and accelerometry [1–3]. Experiments such as are described in Refs. [4–9] are among the most accurate measurements to date of surface gravity and certain fundamental constants [10–12], and also provide probes of general relativity and the inverse square law [4,7,13,14]. Furthermore, accelerometers have wide application in more practical settings such as inertial navigation, vibration detection, and gravitational anomalies such as oil fields [15]. Current experiments use short Raman or Bragg pulses to manipulate spin states followed by periods of free evolution, corresponding to free flight, to accumulate sensitivity to external fields. During free flight, a sensitivity to external fields is imparted on the internal spin states in the form of a path-dependent phase. This phase can then be measured through a final Raman pulse and spin-dependent fluorescence techniques.

At the same time that interferometry has emerged as a tool, interest in synthetic gauge fields has also arisen, mostly in the context of the quantum Hall effect [16,17] and cold atom spintronics [18–21]. These systems use optical coupling of internal spin states, simultaneous with momentum exchange with Raman laser beams, to induce an effective vector potential. Depending on the optical configuration these setups can simulate systems such as spin-orbit coupling [22,23], monopoles [21], or a constant magnetic field [24,25].

The optical coupling to the internal degrees of freedom provides a continuous coupling of momentum and spin. This is in contrast to standard interferometry schemes where spin and momentum coupling is generated only through a set of discrete Raman $\pi/2$ and π pulses. In this paper we propose a new type of interferometer that uses the spin-momentum coupling to measure ac signals. We use the continuous spin-momentum coupling of the gauge field to produce an interferometer sensitive to high-frequency time-dependent (or ac) fields. This is in contrast to current systems whose sensitivity to signals drops above a soft cutoff frequency of $\leqslant 10$ Hz [26,27]. We specifically propose using a trapped system of cold bosons under the influence of an optically induced gauge field to measure weak high-frequency ($\sim$1 kHz) ac gravity signals. We discuss some potential implementations and we estimate that such a system will have a sensitivity of $S \sim 10^{-7}\,\frac{\mathrm{m/s^2}}{\sqrt{\mathrm{Hz}}}$. We note that, since our system is trapped, it can be implemented on an atom chip [28–30].

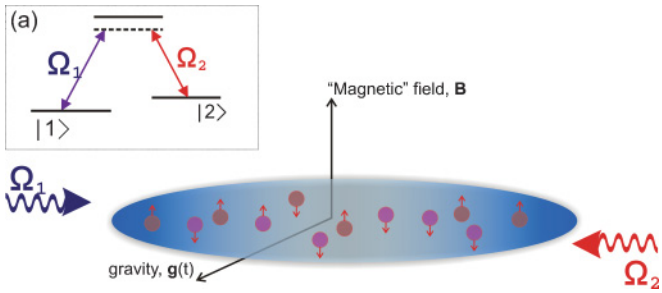

FIG. 1. (Color online) A potential implementation of our interferometer based upon Ref. [17]. The Raman beams Ω_1 and Ω_2 couple a three-level atom by two parallel Gaussian profiles with peaks that are spatially offset. The spatial offset of the beams provides a torque on the atoms that looks like a magnetic field. Two of the dressed states couple to a "synthetic gauge field" with opposite charges and become degenerate in the large detuning limit $\Delta \to \infty$.

As a toy model, we consider a single particle with an internal degree of freedom (pseudospin) in a harmonic trap with spin-orbit coupling and an external force:

$$H = \frac{[\hat{\mathbf{p}} - \sigma \mathbf{A}(\hat{\mathbf{r}})]^2}{2m} + \frac{1}{2} m\omega_0^2 \hat{\mathbf{r}}^2 - m\mathbf{g}(t)\cdot\hat{\mathbf{r}}, \qquad (1)$$

where $\hat{\mathbf{p}}$ and $\hat{\mathbf{r}}$ are the position and momentum operators, respectively, ω_0 is the trapping frequency, $\sigma = \pm 1$ labels the pseudospin of the particle, m is the mass of the particle, $\mathbf{g}(t)$ is the time-dependent external force, and $\mathbf{A}(\hat{\mathbf{r}})$ is the spin-orbit coupling field, or vector potential. We confine the particle to a two-dimensional plane and chose the vector potential to have the form of a magnetic field $\mathbf{A}(\hat{\mathbf{r}}) = m\omega_c x\hat{\mathbf{y}}$, where ω_c is the characteristic frequency scale of the spin-orbit coupling and $\hat{\mathbf{e}}_z$ is the unit vector perpendicular to the plane of confinement. This toy model captures the ideal behavior of systems such as Ref. [17,25].

Without spin-orbit coupling ($\omega_c \to 0$), the path of the particle will depend on the force $\mathbf{g}(t)$ and will be independent of spin. With spin-orbit fields the path will depend on the spin of the particle as well as the force. In an atom interferometer, path differences can be mapped to an interference signal by creating an initial superposition of two spin states and sending them on spin-dependent trajectories. The phase picked up on a semiclassical path can be found by expanding the action S about the classical trajectory in the path integral formulation of quantum mechanics.

For the system in Eq. (1) we find that the first-order phase factor due to $\mathbf{g}$ is

$$e^{iS_g/\hbar} = e^{i\frac{m}{\hbar}\int dt\mathbf{r}(t)\cdot\mathbf{g}(t)}. \tag{2}$$

We become sensitive to this phase by creating an initial spin superposition $\frac{|1\rangle+|-1\rangle}{\sqrt{2}}|\phi\rangle_{\text{orbital}}$, which evolves to $\frac{1}{\sqrt{2}}(e^{iS_1}|1\rangle|\phi_1\rangle + e^{iS_{-1}}|-1\rangle|\phi_{-1}\rangle)$. In general, the spin states $|\pm1\rangle$ are entangled to the orbital states $|\phi_{\pm1}\rangle$. In order to measure the phase we desire a pure spin measurement. We chose the paths to have complete orbital overlap, $\langle\phi_1|\phi_{-1}\rangle = 1$, at the time of phase measurement. This places the system in the pseudospin state $\frac{1}{\sqrt{2}}(|1\rangle + e^{i\Delta S}|-1\rangle)$, which allows us to measure $\Delta S = S_{-1} - S_1$ though a single operator measurement such as $\hat{S}_y$. Note that the $H_{\mathbf{g}=\mathbf{0}}$ contributions to $S_{\pm1}$ are equal, and thus do not lead to interference effects.

The physics described in our toy model is an idealized version of the proposal given in Ref. [17], although other setups such as the experiment by Y. J. Lin *et al.* [25] have similar physics. This setup uses a cold atom in a Λ-scheme, as can be seen in the inset of Fig. 1. The Raman beams used have a Gaussian profile with offset centers which give spatial dependence to the dressed states. This spatial dependence induces dynamics that is identical to a charged particle in a magnetic field. In the large detuning limit $\Delta \to \infty$, one of the bright states becomes degenerate with the dark state; however, the "charge" that these two states see has opposite sign. We note that the synthetic field in this setup is nonuniform. This leads to further technical difficulties but does not change the underlying physics of our proposal.

We now detail the specific solution for our spin-orbit-coupled system described by Eq. (1). We start by solving the Heisenberg equations of motion for the system. These correspond to the classical, spin-dependent Hamilton equations of motion since the system is quadratic in $\mathbf{r}$ and $\mathbf{p}$. Not surprisingly, these solutions correspond to a combination of cyclotron orbits and orbits around the trap center. The direction of the orbits is set by the pseudospin σ.

The solutions are characterized by the two frequencies $\omega_\pm = \tilde{\omega} \pm \omega_c/2$, with $\tilde{\omega}^2 = \omega_0^2 + (\omega_c/2)^2$. We will consider initial conditions given by $\mathbf{r}(0) = \mathbf{r}_0$ and $\dot{\mathbf{r}}(t) = \mathbf{0}$, as will be discussed later. Figure 3(b) shows these paths in the absence of a driving field. The sign of the charge changes the direction of cyclotron motion so the paths are mirrored along $\mathbf{r}_0$. We expect a driving force to break the mirror symmetry of the paths.

In a quantum system this symmetry-breaking perturbation will result in a pseudospin-dependent phase. We can exploit this phase to make an interference measurement. Specifically, we would prepare the system in an initial state $|0,\uparrow\rangle$, where $|0\rangle$ is the orbital ground state of the system and $\sigma_z|\uparrow\rangle = |\uparrow\rangle$. Next we place the system in a superposition of pseudospin states with a $R_{\hat{\mathbf{y}}}(\pi/2) = e^{-i\sigma_y\pi/4}$ Raman pulse. Then, we suddenly displace the minimum of the harmonic trap by an amount $\mathbf{r}_0$. If we allow the system to evolve freely in time, the two different spin states will follow time-reversed classical trajectories. In the process, they also accumulate a pseudospin-dependent phase term $\exp[i\sigma_z(\hat{\mathbf{z}}\times\mathbf{r}_0)\cdot\int dt\,\mathbf{g}(t)h_\perp(t)]$, where $h_\perp(t) = \frac{1}{2\tilde{\omega}}[\omega_-\sin(\omega_+t) - \omega_+\sin(\omega_-t)]$. We now wait for a time t at which the two classical trajectories overlap again. We then use a $R_{\hat{\mathbf{y}}}(-\pi/2)$ pulse to convert the coherence into a population. An S_z-spin measurement will give

$$\langle S_z\rangle = \sin\left[2\int_0^{t'} dt\,(\hat{\mathbf{z}}\times\mathbf{r}_0)\cdot\mathbf{g}(t')h_\perp(t')\right]. \tag{3}$$

where we have neglected higher-order terms in $g/(l_o\omega^2)$ with the harmonic oscillator length $l_o = \sqrt{\hbar/(m\tilde{\omega})}$. We can represent the above pulse sequence as the unitary matrix $U_p = R_{\hat{\mathbf{y}}}(-\pi/2)U(t)D[R\mathbf{r}_0]R_{\hat{\mathbf{y}}}(\pi/2)$ where $D[\mathbf{r}_0]$ is a spatial displacement of $\mathbf{r}_0$ and the time evolution operator $U(t)$ can be found exactly. The expectation value in Eq. (3) is then given by $\langle S_z\rangle = \langle 0,\uparrow|U_p^\dagger S_z U_p|0,\uparrow\rangle$ and can be shown to reproduce Eq. (3).

We now find the response of our interferometer to an arbitrary time-varying force. We can express our spin population measurement as $\langle S_z\rangle = \sin[\int\frac{d\omega}{2\pi}\tilde{g}_\perp(\omega)F_0(\omega)]$ where $\mathbf{g}(t) = \int\frac{d\omega}{2\pi}e^{-i\omega t}\tilde{\mathbf{g}}(\omega)$ and

$$F_0(\omega) = \frac{ir_0t}{\tilde{\omega}}\sum_{\{\sigma,\tau=\pm1\}}\sigma\tau\omega_{-\sigma}f(\omega+\tau\omega_\sigma) \tag{4}$$

is the response function of the system, where $f(\omega) = \frac{\sin(\omega t/2)}{\omega t/2}e^{-i\omega t/2}$. The behavior of the response function can be seen in Fig. 2. The peak response of the system is at the frequencies $\omega = \omega_\pm$ with relative peak amplitudes of ω_-/ω_+. The bandwidth of the system varies with $1/t$, giving a large bandwidth at small times. Note that our system is sensitive to dc signals since $F(\omega)$ is finite for $\omega \to 0$. For the purposes of this paper this dc sensitivity is unwanted, and we will discuss methods of dealing with it later.

It is important to note that we have waited until the coherent states overlap fully. A measurement at a different time would suppress our signal by a factor of $A = e^{-[2\frac{r_0}{l_o}h_\perp(t)]^2}$. The double-exponential suppression thus requires that we obtain as complete an overlap as possible. We can eliminate dc signals while simultaneously improving the overlap and eliminating

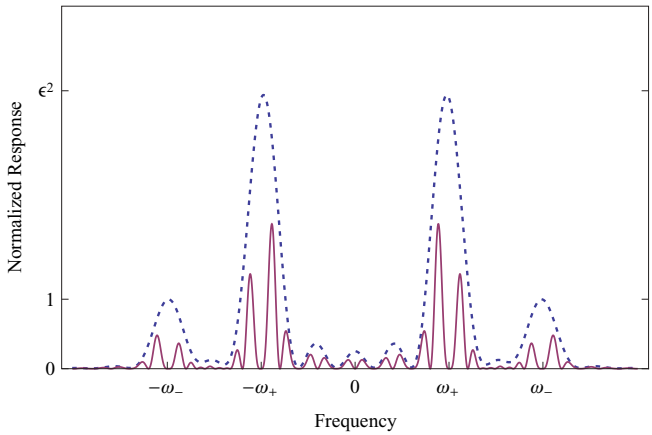

FIG. 2. (Color online) The normalized response function for $|\frac{\tilde{\omega}F(\omega)}{r_0t}|^2$ for the pulse sequence U_p, (dashed) or U_{CP}, the Carr-Purcell-like pulse sequence (solid). For both sequences we used $t = \frac{10\pi}{\omega_+ + \omega_-} = \frac{5\pi}{\tilde{\omega}}$ and $\epsilon = \omega_+/\omega_-$. Note we have scaled the response for the Carr-Purcell pulse sequence by a factor of 16 to account for the factor-of-four increase in interrogation time.

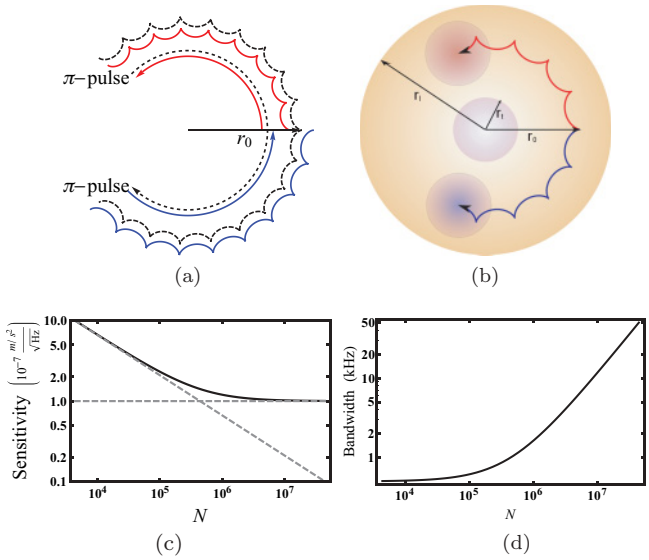

FIG. 3. (Color online) (a) Classical path a particle will follow with the CP pulse sequence given by Eq. (5). The red path corresponds to the initial free evolution for a time t. The dashed path is the time-reversed path allowed to evolve for a time $2t$. Finally, the solid blue path is the return trajectory for another t. Note that the three trajectories will overlap in practice, and have been offset just for a visual aid. The three arcs correspond to the direction of motion of the classical trajectory. We have also chosen $\epsilon = \omega_+/\omega_- = 22$. (b) Schematic of the experimental setup. A thermal cloud of radius r_t is displaced by $r_0 = r_l - r_t$, which is limited by the laser-inhomogeneity radius r_l. The two spin states orbit along trajectories mirrored across $\mathbf{r}_0$. (c) Dependence of the sensitivity of the system based upon atom number. Below $N_c \sim 10^6$ the sensitivity grows as $\frac{1}{\sqrt{N/N_c}}$. Above N_c the sensitivity $S \sim 10^{-7}(\mathrm{m/s^2})/\sqrt{\mathrm{Hz}}$ is independent of the number of particles. (d) Bandwidth of the system with optimal sensitivity as a function of the number of particles.

other sources of error through application of $R_{\hat{\mathbf{y}}}(\pi)$ pulses in a sequence analogous to the Carr-Purcell (CP) pulse sequence in NMR [31]. If applied at a time when the velocity vanishes, a π pulse will time reverse the particle's motion, causing it to retrace its path. Such a time is guaranteed and occurs at time intervals of $t = \frac{2\pi n}{\omega_+ + \omega_-} = \frac{\pi n}{\tilde{\omega}}$. If we wait for an additional time $2t$ after the first π pulse to apply a second π pulse, the path will be time reversed again and return to the origin. It is clear that any dc signals will be canceled by such a pulse sequence as the path returns to itself, so the average position is zero. We note that this pulse sequence will also help to cancel certain noise sources such as Zeeman fields or small trapping asymmetries.

In the operator language such a pulse sequence has the form

$$U_{\mathrm{CP}} = R_{\hat{\mathbf{y}}}(-\pi/2)U(t)R_{\hat{\mathbf{y}}}(\pi)U(2t)R_{\hat{\mathbf{y}}}(\pi)U(t)D[R\mathbf{r}_0]R_{\hat{\mathbf{y}}}(\pi/2). \tag{5}$$

Application of such a pulse sequence modifies the response function to

$$F(\omega) = 2i\,\sin(\omega t)[F_0(\omega)e^{i\omega t} + F_0^*(\omega)e^{-i\omega t}]e^{i2\omega t}, \tag{6}$$

where $F_0(\omega)$ is the response function given in Eq. (4). The complex conjugate term $F_0^*(\omega)$ arises due to the time reversal of the paths. This response function is plotted in Fig. 2. The new response function now vanishes at $\omega = 0$ and $\omega = \omega_\pm$; however we still have large sensitivity in the frequency range $\omega = \frac{1}{8}\frac{2\pi}{t}$ around $\omega_\pm$.

We now generalize from a single particle to a thermal ensemble of ultracold dilute atoms in the presence of an induced spin-orbit Hamiltonian of the form shown in Eq. (1). From a practical standpoint, a system of dilute cold atoms allows us to neglect complications arising from atom-atom interactions in a Bose-Einstein condensate (BEC). Consider a thermal ensemble of cold atoms at a temperature T. Using the Glauber P-representation [32], the density matrix has the form $\rho = \int d\boldsymbol{\alpha}\, e^{-|\alpha_+|^2/\langle n_+\rangle - |\alpha_-|^2/\langle n_-\rangle}|\boldsymbol{\alpha}\rangle\langle\boldsymbol{\alpha}|$, where $\langle n_i\rangle = [\exp(\hbar\omega_i/kT) - 1]^{-1}$ is the average occupation for the classical mode of frequency ω_i. Such an ensemble suppresses the expectation value of the S_z operator by a factor $e^{-\langle n_+\rangle|\gamma_+|^2 - \langle n_-\rangle|\gamma_-|^2}$ relative to the single-particle or zero-temperature expectation value. The suppression factor $\gamma_\pm$ depends on the pulse sequence used. For example, using the pulse sequence U_p given above we get $\gamma_+ = \frac{l_o}{2}\int_0^t dt'\,(g_x + ig_y)e^{i\omega_+ t'}$ and $\gamma_- = \frac{l_o}{2}\int_0^t dt'\,(g_y + ig_x)e^{i\omega_- t'}$. Note that we can express $\int dt\,\mathbf{r}\cdot\mathbf{g}$ as a superposition of γ_+ and γ_-. For the Carr-Purcell-like pulse sequence the suppression factor $\gamma_\pm$ is more complicated, but can still form a basis for which we can express the phase. This implies that $\gamma_\pm$ has a similar frequency dependence to $F(\omega)$.

We are now in a position to discuss the measurement capabilities of such a system. We first estimate the maximum ac signal such a system can measure. To avoid signal suppression due to the finite temperature of the ensemble, we bound the maximum strength of ac signals our system can measure by $g_{\max} \leqslant \frac{1}{\sqrt{\langle n\rangle}}\frac{4\pi\hbar}{mr_0\tau}$. In this limit the sensitivity for our detector can be estimated with

$$S \sim \sqrt{\frac{1}{N\tau}}\frac{2\pi\hbar}{mr_0}, \tag{7}$$

where the lifetime of one measurement, $1/\tau = \gamma_{\mathrm{SE}} + \gamma_{\mathrm{coll}}$ is limited by spontaneous emission γ_{SE} and collisions γ_{coll}.

To maximize the system's sensitivity to accelerations (or minimize S), we need to consider the effect of collisions and the spatial configuration of the system. We desire to confine our system to a "laser-homogeneity" radius r_l, for which nonlinear variations in the laser fields are suppressed. The effective two-dimensional system will use an axial trapping potential of $\omega_\parallel \geqslant \ln(2)kT/\hbar$ to freeze all motion into a single transverse mode. Thus our system will have $N_l = r_l/d$ layers, where $d = \sqrt{\hbar/(m\omega_\parallel)}$, providing for an increase in sensitivity of $1/\sqrt{N_l}$. The radius r_l further constrains our sensitivity by bounding the maximum trap displacement by $r_0 = r_l - r_t$, where $r_t = \sqrt{\langle n\rangle}l_o \sim \langle v\rangle/\tilde{\omega}$ is the thermal radius of a thermal ensemble and $\langle n\rangle = kT/(\hbar\omega)$ and $\langle v\rangle = \sqrt{3kT/m}$ are the respective high-temperature thermal occupation number and velocity [Fig. 3(b)].

The lifetime of the system will be dominated by spontaneous emission at low densities and collisions at high densities. To optimize the sensitivity we desire to place as many atoms per layer as possible. The collisional scattering rate is given by $\gamma_{\mathrm{coll}} = \frac{N_a\langle v\rangle a^2}{dr_t^2}$, where a is the interparticle scattering length. The critical number of atoms at which the collision rate begins

to dominate the spontaneous emission rate is $N_c = \frac{\langle v \rangle a^2}{\gamma_{SE} d r_l^2}$. We see that, in the small-atom-number limit, the sensitivity is a monotonically decreasing function of the trapping frequency and has a $1/\sqrt{N_a}$ dependence. However, in the large-atom limit the sensitivity is minimized at a trapping frequency of $\omega_{\min} = 2\langle v \rangle / r_l$ and the sensitivity becomes independent of the number of atoms per layer. Note that, in this limit the bandwidth of the system is increased by adding atoms [see Fig. 3(d)].

We assume our thermal ensemble has a temperature of $T \sim 1\ \mu$K with a frequency scale $\tilde{\omega} = 2\pi$ kHz. At these temperatures the gas is nondegenerate and is described well by a classical gas. For this temperature we find an upper bound of $g \sim 10^{-2} \mathrm{m/s^2}$ before exponential suppression of the signal above becomes relevant. We will consider a cold gas of ^{87}Rb cooled to $T = 1\ \mu$K with an axial confinement distance of $d = 1\ \mu$m. We take the spontaneous emission rate to be $\Gamma_{SE} = 1/70\ \mathrm{ms}^{-1}$ [23] and the laser-inhomogeneity radius to be $r_l = 10$–$25\ \mu$m. In the $N_a \gg N_c$ limit we estimate the sensitivity to be $S \sim 10^{-7} \frac{\mathrm{m/s^2}}{\sqrt{\mathrm{Hz}}}$. A similar analysis for a three-dimensional system gives a sensitivity drop of approximately an order of magnitude. We note that, had we instead used a fermionic species, we would obtain a similar result since we have two spin species.

The concept of a continuous coupling of spin to momentum can also be extended to a continuous coupling of spin and position. We note that, in a harmonic trap, position and momentum are dual variables, and thus a spin-dependent term in the Hamiltonian that has spatial variation will experience a similar phase accumulation to the system described above. An example would be a trapped spin-1 system in the presence of a Zeeman field with a strong spatial variation. In such a system the Zeeman field will act to trap (antitrap) the $S_z = +1$ and $S_z = -1$ spin states with different trapping potentials. This will play a similar role to the opposite charge couplings to gauge fields given above. However, such a system requires strong magnetic field gradients so it may be impractical.

Finally, we note that this system is not limited to measurements of ac signals. Through appropriate modifications of pulse sequences such a scheme is capable of measurements of dc gravity and gravitational gradients and rotations. Due to electronics noise, the sensitivity of these systems will be significantly lower than existing atom interferometers. However, for some applications they may still be useful due to the ability to place the system on a chip.

This research was supported by the JQI Physics Frontiers Center. B.M.A. and V.M.G. acknowledge support from US-ARO and J.M.T. was supported through ARO-MURI-W911NF0910406. The authors are grateful to Ian Spielman for illuminating discussions.

[1] J. F. Clauser, Physica B + C **151**, 262 (1988).
[2] M. de Angelis *et al.*, Meas. Sci. Technol. **20**, 022001 (2009).
[3] A. Cronin, J. Schmiedmayer, and D. E. Pritchard, Rev. Mod. Phys. **81**, 1051 (2009).
[4] S. Dimopoulos, P. W. Graham, J. M. Hogan, and M. A. Kasevich, Phys. Rev. Lett. **98**, 111102 (2007).
[5] A. Peters, K. Y. Chung, and S. Chu, Nature (London) **400**, 849 (1999).
[6] A. Peters, K. Y. Chung, and S. Chu, Metrologia **38**, 25 (2001).
[7] S. Dimopoulos, P. W. Graham, J. M. Hogan, and M. A. Kasevich, Phys. Rev. D **78**, 042003 (2008).
[8] M. Snadden, J. M. McGuirk, P. Bouyer, K. G. Haritos, and M. A. Kasevich, Phys. Rev. Lett. **81**, 971 (1998).
[9] J. McGuirk, G. T. Foster, J. B. Fixler, M. J. Snadden, and M. A. Kasevich, Phys. Rev. A **65**, 033608 (2002).
[10] J. B. Fixler *et al.*, Science **315**, 74 (2007).
[11] M. J. Biercuk *et al.*, Nature Nanotechnology **5**, 646 (2010).
[12] A. Bertoldi *et al.*, Eur. Phys. J. D **40**, 271 (2006).
[13] H. Müller, S. W. Chiow, S. Herrmann, S. Chu, and K. Y. Chung, Phys. Rev. Lett. **100**, 031101 (2008).
[14] T. van Zoest *et al.*, Science **328**, 1540 (2010).
[15] A. B. Chatfield, *Fundamentals of High Accuracy Inertial Navigation* (American Institute of Aeronautics and Astronautics, 1997).
[16] G. Juzeliūnas, J. Ruseckas, P. Ohberg, and M. Fleischhauer, Phys. Rev. A **73**, 025602 (2006).
[17] S. L. Zhu, H. Fu, C. J. Wu, S. C. Zhang, and L. M. Duan, Phys. Rev. Lett. **97**, 240401 (2006).
[18] T. D. Stanescu, C. Zhang, and V. M. Galitski, Phys. Rev. Lett. **99**, 110403 (2007).
[19] L.-H. Lu and Y.-Q. Li, Phys. Rev. A **76**, 023410 (2007).
[20] X.-J. Liu, M. F. Borunda, X. Liu, and J. Sinova, Phys. Rev. Lett. **102**, 046402 (2009).
[21] J. Ruseckas, G. Juzeliunas, P. Ohberg, and M. Fleischhauer, Phys. Rev. Lett. **95**, 010404 (2005).
[22] T. D. Stanescu, B. Anderson, and V. Galitski, Phys. Rev. A **78**, 023616 (2008).
[23] Y. J. Lin *et al.*, Phys. Rev. Lett. **102**, 130401 (2009).
[24] I. B. Spielman, Phys. Rev. A **79**, 063613 (2009).
[25] Y. J. Lin *et al.*, Nature (London) **462**, 628 (2009).
[26] S. Dimopoulos, P. W. Graham, J. M. Hogan, M. A. Kasevich, and S. Rajendran, Phys. Rev. D **78**, 122002 (2008).
[27] M. Hohensee *et al.*, e-print arXiv:1001.4821.
[28] Y. Shin *et al.*, Phys. Rev. Lett. **92**, 050405 (2004).
[29] T. Schumm *et al.*, Nature Phys. **1**, 57 (2005).
[30] W. Hänsel, J. Reichel, P. Hommelhoff, and T. W. Hansch, Phys. Rev. A **64**, 063607 (2001).
[31] H. Y. Carr and E. Purcell, Phys. Rev. **94**, 630 (1954).
[32] R. Glauber, Phys. Rev. **131**, 2766 (1963).